

[Home](#) [Search](#) [Collections](#) [Journals](#) [About](#) [Contact us](#) [My IOPscience](#)

## Multiple scattering in dispersions, for long wavelength thermoacoustic solutions

This content has been downloaded from IOPscience. Please scroll down to see the full text.

2014 J. Phys.: Conf. Ser. 498 012005

(<http://iopscience.iop.org/1742-6596/498/1/012005>)

View [the table of contents for this issue](#), or go to the [journal homepage](#) for more

Download details:

IP Address: 85.255.234.222

This content was downloaded on 07/09/2015 at 15:31

Please note that [terms and conditions apply](#).

# Multiple scattering in dispersions, for long wavelength thermoacoustic solutions

T A Hazlehurst<sup>1</sup>, O G Harlen<sup>1</sup>, M J Holmes<sup>2</sup> and M J W Povey<sup>2</sup>

<sup>1</sup>Department of Applied Mathematics, University of Leeds, Leeds, LS2 9JT, UK

<sup>2</sup> School of Food Science and Nutrition, University of Leeds, Leeds, LS2 9JT, UK

E-mail: mm07tah@leeds.ac.uk

**Abstract.** Thermoacoustic scattering is a principal scattering mechanism in the ultrasonic characterisation of water-continuous colloids. Thermal effects are particularly important in highly concentrated systems, where non-propagational thermal fields surrounding the disperse particles overlap. For low concentrations, the single sphere solution of Epstein and Carhart has become a popular tool for determining the particle size distribution. However, for small particle sizes it suffers from ill-conditioning that can make the solution numerically unstable. This problem has been resolved, by Harlen *et al.* (2001, SIAM Journal on Applied Mathematics, **61** 1906–1931), who obtained an asymptotic solution for low concentrations that is valid when the particle diameter is small compared to the wavelength. In this paper we will use this asymptotic method to calculate the effects of multiple scattering that occur at higher concentrations. We use the addition translation theorem to calculate the effects of multiple scattering between a pair of spheres of different sizes and show how this affects the close-field scattering pattern.

## 1. Introduction

Ultrasonic techniques are becoming increasingly popular tools for characterising soft solids and colloids. In particular, ultrasound spectroscopy can be used to measure non-intrusively particle sizes within opaque materials in food, chemical and pharmaceutical manufacturing, where other techniques, such as, light scattering, are ineffective.

The first theory of ultrasound propagation in dispersions was developed by Lord Rayleigh [1]. This theory was then extended to fog and solid particles by Epstein and Carhart [2] and Allegra and Hawley [3], respectively. In thermoacoustic scattering the sound wave is scattered by the differences in thermal properties between the phases. The transmission problem reduces to the solution of a pair of coupled Helmholtz equations for the acoustic and thermal scattering fields. The acoustic field describing the scattered sound, with wavenumber  $k_c$ , while the thermal field represents the temperature fluctuations near the droplet boundaries and has a complex wavenumber  $k_T$ . This thermal wave decays rapidly with distance and the inverse of  $|k_T|$  represents the distance heat can diffuse over the period of the radiation.

The ECAH (Epstein and Carhart and Allegra and Hawley) calculation does not account for multiple scattering within a suspension and so only provides accurate solutions for low concentrations. Lloyd and Berry [4] developed a method of including multiple scattering based on an infinite number of energy shells. However this method is only applied to the acoustic field and so does not consider the changes to the scattering from the overlap of the thermal fields between neighbouring droplets. Gaunaurd, Huang and Strifors [5] have formulated a method



for calculating the scattering from a pair of spheres of different sizes at arbitrary angles to the incidence wave. They make use of the translation addition theorem to determine the secondary scattering of the scattered acoustic wave from a neighbouring sphere.

For the case of the scattering of a plane wave by a single spherical droplet, an analytical solution of the ECAH can be obtained as an infinite sum of spherical Bessel and Hankel functions. However, in the long acoustic wavelength limit  $k_c a \ll 1$  (where  $a$  is the particle radius), typical of many colloids, the solution for the coefficients is ill-conditioned [6]. However by treating  $k_c a$  as a small parameter, a regular perturbation solution can be found that converges rapidly on the solution [6–8].

In this paper we use this perturbation approach to address the multiple thermoacoustic scattering between a pair of spherical droplets. In section 4, we consider how the thermal fields interact when the spheres are within a distance of  $1/|k_T|$  of one another. This is then used to correct the far-field scattering pattern from which the attenuation is calculated. In section 5 we discuss how the accuracy of the coefficients of the far-field scattering pattern depends upon the number of terms used in the near field expansions, particularly when the spheres are close.

## 2. Motivation

The motivation behind this work is the need to develop a theory for thermoacoustic scattering in colloids that is accurate for high concentrations. In figure (1) we compare the attenuation predicted by the ECAH theory with that measured in monodisperse silicon oil-in-water emulsions for concentrations ranging from 5 to 50 %. While the model is reasonably accurate at the lower concentrations. For concentrations above 20% the theory substantially over-predicts the attenuation. Furthermore, applying the correction of Lloyd and Berry does not correct this.

The explanation of this discrepancy can be found by examining the decay length of the thermal field around the oil droplets, which is given by [9] as

$$\delta_T = \sqrt{\frac{2\tau}{\rho C_p \omega}}, \quad (1)$$

where  $\tau, \rho, C_p$  and  $\omega$  are thermal conductivity, density, specific heat capacity and angular frequency respectively. At low concentrations the droplets are sufficiently far enough apart that these fields don't interact. However if

$$\delta_T \geq \frac{d}{2}, \quad (2)$$

where  $d$  is the distance between the centre of neighbouring droplets, then the thermal field of two droplets will overlap. From this we can define the critical concentration  $\phi_C$  at which the thermal fields between neighbouring particles will overlap. This critical volume fraction is given by [10]

$$\phi_C = \left( \frac{1}{1 + \frac{\delta_T}{a}} \right)^3, \quad (3)$$

which for the case of the experimental in figure (1) is approximately 18%.

## 3. Low Frequency Thermoacoustic scattering

In thermoacoustic scattering the scattered field is written as the sum of an acoustic and a thermal wave so that the velocity potential is given by  $e^{ik_c z} + \varphi + \psi$  in the continuous phase and  $\varphi' + \psi'$  in the suspended phase, where  $e^{ik_c z}$  is the incident plane wave,  $\varphi$  and  $\varphi'$  are the

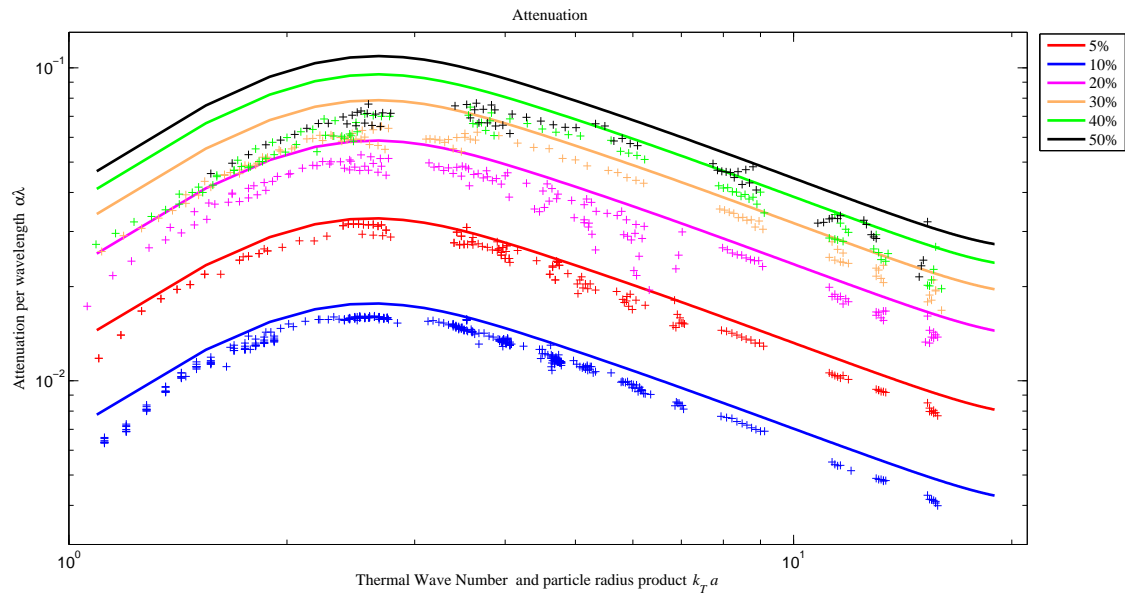


**Figure 1.** Attenuation spectrum based on the ECAH approach for a silicone oil-in-water emulsion of particle radius  $0.23\mu\text{m}$  for different concentrations. It can be seen that when the concentration rises above the critical volume fraction  $\phi_C$  given in (3) (in this case  $\phi_C = 18\%$ ) the theory significantly overpredicts the attenuation. Experimental data from Herrmann [11].

scattered acoustic fields in the two phases and  $\psi$  and  $\psi'$  the thermal fields. Each of the four fields satisfies a Helmholtz equations [2],

$$(\nabla^2 + k_c^2) \varphi = 0, \quad (\nabla^2 + k_T^2) \psi = 0 \quad \text{in the continuous phase}, \quad (4)$$

and

$$(\nabla^2 + k_c'^2) \varphi' = 0, \quad (\nabla^2 + k_T'^2) \psi' = 0 \quad \text{in the droplet phase}, \quad (5)$$

where the acoustic and thermal wave numbers are given by  $k_c = \frac{\omega}{c} (1 + i\alpha)$  and  $k_T = (1 + i)\sqrt{\frac{\omega}{2\sigma}}$ , respectively. Here  $c, \alpha$  and  $\sigma$  are the wave speed, attenuation coefficient and the thermometric conductivity.

The thermal and acoustic waves are coupled through the boundary conditions at the phase boundaries, where we have continuity of:

Normal velocity

$$\frac{\partial}{\partial n} (e^{ik_c z} + \varphi + \psi) = \frac{\partial}{\partial n} (\varphi' + \psi'), \quad (6)$$

Pressure

$$e^{ik_c z} + \varphi + \psi = \hat{p}(\varphi' + \psi'), \quad (7)$$

Temperature

$$\Gamma_c (e^{ik_c z} + \varphi) + \Gamma_t \psi = \Gamma_c' \varphi' + \Gamma_t' \psi', \quad (8)$$

Heat flux

$$\Gamma_c \frac{\partial}{\partial n} (e^{ik_c z} + \psi) + \Gamma_t \frac{\partial}{\partial n} \psi = \hat{\tau} \left( \Gamma'_c \frac{\partial}{\partial n} \varphi' + \Gamma'_t \frac{\partial}{\partial n} \psi' \right), \quad (9)$$

where  $\Gamma_c, \Gamma'_c, \Gamma_T$  and  $\Gamma'_T$  are as described in [8].

In most applications the radius of colloidal particles is much smaller than the length of the acoustic waves, so that  $|k_c a| \ll 1$ . For this low frequency limit we can follow the approach of Harlen *et al.* [8], and find a perturbation solution for the limit when the acoustic wavelength is large compared to droplet radius,  $k_c a \ll 1$  but where the width of the thermal  $\delta_T$  is comparable with particle radius so that  $|k_T a| \sim 1$ .

The external Helmholtz equation (4) is first transformed by defining,

$$\tilde{\varphi} = e^{-ik_c(r-a)} \varphi. \quad (10)$$

where  $r$  is radial distance from the origin, to give a regular problem at infinity, allowing us to seek regular perturbation solution as power series in  $ik_c a$ ,

$$(\tilde{\varphi}, \varphi', \psi, \psi') = \sum_{n=0}^{\infty} (ik_c a)^n (\tilde{\varphi}_n, \varphi'_n, \psi_n, \psi'_n) \quad (11)$$

This series converges provided  $|k_c a| < \ln(2)$  [13] and converges rapidly, giving accurate answers with just a few terms, when  $|k_c a| \ll 1$  [8]. Substituting the expansion into the Helmholtz equations (4) gives the following system, for  $n \geq 0$ ,

$$\nabla^2 \tilde{\varphi}_n = -\frac{2}{ar} \frac{\partial}{\partial r} (r \tilde{\varphi}_{n-1}), \quad \text{for the continuous phase} \quad (12)$$

and

$$\nabla^2 \varphi'_n = \left( \frac{k'_c}{k_c} \right)^2 \varphi'_{n-2}, \quad \text{for the dispersed phase.} \quad (13)$$

The thermal fields remain given by Helmholtz equations with

$$(\nabla^2 + k_T^2) \psi_n = 0, \quad \text{in the continuous phase} \quad (14)$$

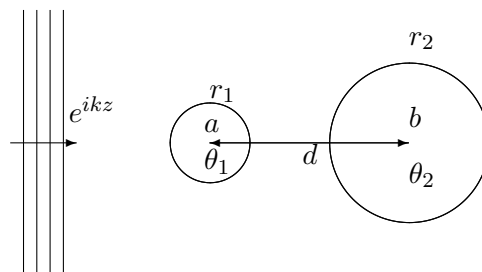


**Figure 2.** Set up for the two particle problem with a plane wave travelling parallel to the placement of two different sized spheres of radii  $a$  and  $b$  respectively separated by a distance  $d$ . We have a plane wave described by  $e^{ik_c z}$  where  $z$  is the coordinate along the axis of the particle centres and  $r_1, \theta_1$  and  $r_2, \theta_2$  denote the polar coordinates with the origin based on centres of the spheres 1 and 2 respectively.

and

$$(\nabla^2 + k_T'^2) \psi'_n = 0, \quad \text{in the dispersed phase} \quad (15)$$

The boundary conditions at the phase boundaries can be grouped into pairs. The pressure and normal velocity boundaries give one pair relating  $\tilde{\varphi}_n, \varphi'_n, \psi_n$  and  $\psi'_n$ , where the thermal conditions gives relations between  $\tilde{\varphi}_{n-2}, \varphi'_{n-2}, \psi_n$  and  $\psi'_n$ , where  $\psi_0 = \psi_1 = \psi'_0 = \psi'_1 = 0$ . From this solutions can be calculated sequentially in the order,  $\{\tilde{\varphi}_0, \varphi'_0\}, \{\tilde{\varphi}_1, \varphi'_1\}, \{\psi_2, \psi'_2\}, \{\tilde{\varphi}_2, \varphi'_2\}, \{\psi_3, \psi'_3\}, \dots$ . At order  $n = 0$  the solution is simply  $\{\tilde{\varphi}_0 = 0, \varphi'_0 = 1/\hat{\rho}\}$ .

#### 4. Low frequency thermoacoustic scattering by two spherical droplets

We now consider the thermoacoustic scattering solutions for two spheres, which for simplicity we assume are arranged parallel to the direction of the incident wave, separated by a distance  $d$ , as shown in figure (2). We use two polar coordinate systems, denoted by  $(r_1, \theta_1)$  and  $(r_2, \theta_2)$  centred on particles 1 and 2 respectively.

Following the method of Gaunaurd [5], we express the thermal wave in the continuous phase as the sum of two spherical wave expansions centred on the particle centres. Since we have chosen the particles to lie along the axis of the incident wave the solution is axisymmetric so that we only need to retain the  $p = 0$  terms (the more general case is given in reference [5]), so that

$$\psi_n = \sum_{q=0}^{\infty} \left[ A_{nq} h_q^{(1)}(k_T r_1) P_q(\cos \theta_1) + B_{nq} h_q^{(1)}(k_T r_2) P_q(\cos \theta_2) \right] \quad (16)$$

As we also need to consider the boundaries around both particles, the solution needs to be expressed solely in terms of  $r_i$  and  $\theta_i$ , where  $i = 1, 2$  depending on whether we are considering solutions about the first sphere, (1), say, or the second sphere, (2). To do this we use the translation theorem to express the solution in terms of coordinates centred about particle A,

$$\psi_n^{(1)} = \sum_{q=0}^{\infty} \left[ C_{nq} h_q^{(1)}(k_T r_1) + D_{nq} \sum_{m=0}^{\infty} Q_{T(qm)}^{(2)}(d) j_q(k_T r_1) \right] P_q(\cos \theta_1), \quad (17)$$

where

$$Q_{T(qm)}^{(2)}(d) = i^{q-m} (2q+1) \sum_{\sigma=|q-m|}^{q+m} i^{\sigma} b_{\sigma}^{(qm)} h_{\sigma}^{(1)}(k_T d), \quad (18)$$

and

$$b_{\sigma}^{(qm)} = (2\sigma+1) \begin{pmatrix} q & m & \sigma \\ 0 & 0 & 0 \end{pmatrix}^2, \quad (19)$$

where the Wigner  $3-j$  symbols are defined by [12]. Similarly, about the second particle (2),

$$\psi_n^{(2)} = \sum_{q=0}^{\infty} \left[ D_{nq} h_q^{(1)}(k_T r_2) + C_{nq} \sum_{m=0}^{\infty} (-1)^{q+m} Q_{T(qn)}^{(2)}(d) j_q(k_T r_2) \right] P_q(\cos \theta_2). \quad (20)$$

The thermal fields inside particle ( $i$ ) are given by

$$\psi_n^{(i)} = \sum_{q=0}^{\infty} c_{nq}^{(i)} j_q(k_T r_i) P_q(\cos \theta_i). \quad (21)$$

The solution for the external acoustic field can be written as

$$\tilde{\varphi}_n = \sum_{q=0}^{\infty} A_{nq} \left( \frac{a}{r_1} \right)^{q+1} P_q(\cos \theta_1) + \sum_{q=0}^{\infty} B_{nq} \left( \frac{b}{r_2} \right)^{q+1} P_q(\cos \theta_2) + I_n, \quad (22)$$

where  $I_n$  is a particular solution of the inhomogeneous equation and for  $n = 0$  and  $n = 1$ ,  $I_n = 0$ . Again we can use the translation theorem to express this in terms of the coordinate system around particle (1) as

$$\tilde{\varphi}_n^{(1)} = \sum_{q=0}^{\infty} \left[ A_{nq} \left( \frac{a}{r_1} \right)^{q+1} + B_{nq} \sum_{m=0}^{\infty} Q_{c(qm)}^{(2)} \left( \frac{r_1}{a} \right)^{q+1} \right] P_q(\cos \theta_1) + I_n, \quad (23)$$

and internally in sphere (1)

$$\varphi_n^{(1)} = \sum_{m=0}^{\infty} a_{nq}^{(1)} \left( \frac{r_1}{a} \right)^q P_q(\cos \theta_1) + I_n^{(1)}, \quad (24)$$

where  $I_n^{(1)}$  is a particular solution of the inhomogeneous equation, where  $I_0^{(1)} = I_1^{(1)} = 0$ ,  $I_2^{(1)} = k_c'^2/k_c^2 a^2 \hat{p}$ . Together with the equivalent equations centred on particle (2). Applying the boundary conditions at the particle interfaces gives a system of linear equations for the unknowns  $A_{nq}$  and  $B_{nq}$  or  $C_{nq}$  and  $D_{nq}$ .

## 5. Results

Solving these systems allows us to study the close field interactions between the particles, as seen in figures 3 through 6. In figure 3 we show thermal field for the case of a 200nm and a 1  $\mu\text{m}$  particle. The black dashed lines show the extent of the thermal field  $\delta_T$  around each particle. In this case the thermal field of the smaller particle is engulfed by the field of the larger particle. Consequently the scattering is dominated by the larger particle.

In figure 4 to 6 we show how the thermal field around two particles of equal size (1  $\mu\text{m}$ ) varies as the particle separation changes. In figure 4 the proximity of the particles to each other means that there is heavy overlapping of the thermal fields. As a consequence the total thermal field appears equivalent to that of a single larger particle. This reduces the acoustic attenuation from that of two isolated particles.

The two particles are separated a little further apart in figure 5, with just a small overlap of the thermal fields. However, there are still significant particle-particle interactions mediated through the thermal field. Finally, we can see in figure 6 the particles are much further apart. In this case the thermal field is approximately equal to that of the superposition of the thermal fields from two isolated particles so that the two particles are not coupled thermally.

One issue with solving the linear systems given by applying the boundary conditions to the expansions given in equations (17) and (23) is the number of terms in  $q$  required to obtain an accurate solution. Figures 7 and 8 show the errors in the terms  $A_{20}$  and  $A_{22}$  of the acoustic field respectfully, which are the terms that dominate the far field scattering pattern. When the particles are well separated only a small number of terms are required to give an accurate answer. In these cases the coupling is through the acoustic field. As expected, it can be seen that when the particles are closer together that a larger number of terms are required to give an accurate answer. However, even in the limit  $d = 2a$  when particles are in contact with one another the series converge and can be computed with a moderate number of terms.

## 6. Conclusion

We have demonstrated how the perturbation solution for solving thermoacoustic scattering in the long wave limit can be applied to the scattering by two closely separated spherical particles. This allows us to examine the extent of overlapping of the thermal fields and hence estimate the degree to which the overlapping of thermal fields reduces the thermoacoustic attenuation in a concentrated colloid. The next step is to generalise these results to multiparticles at a

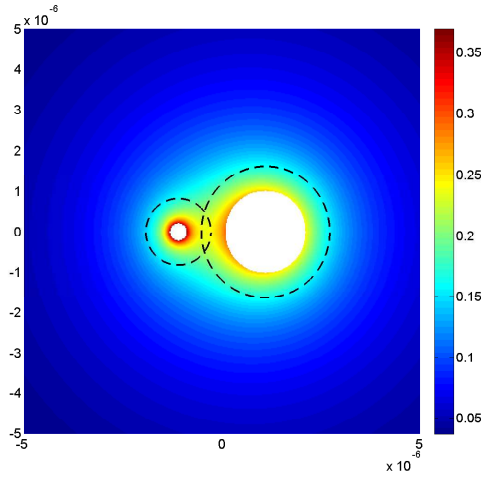


**Figure 3.** The thermal field of two particles,  $a = 2 \cdot 10^{-7}m$ ,  $b = 1 \cdot 10^{-6}m$  and  $d = 2b$ . The black circles show the thermal wave decay described in (1).

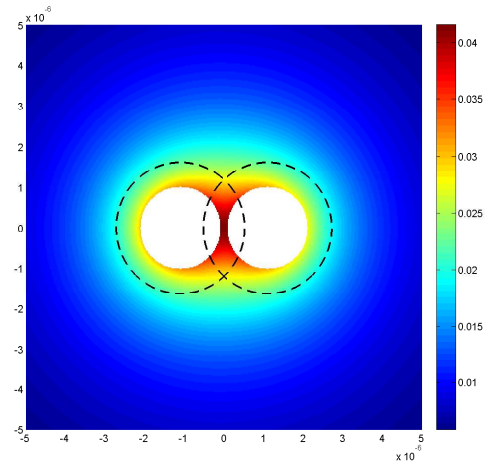


**Figure 4.** The thermal field of two particles,  $a = 1 \cdot 10^{-6}m$ ,  $b = 1 \cdot 10^{-6}m$  and  $d = 2.2a$ . The black circles show the thermal wave decay described in (1).

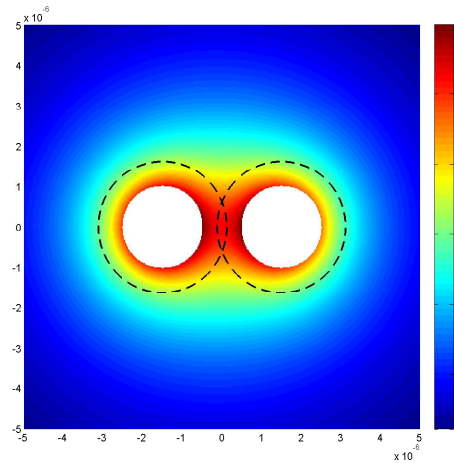


**Figure 5.** The thermal field of two particles,  $a = 1 \cdot 10^{-6}m$ ,  $b = 1 \cdot 10^{-6}m$  and  $d = 3a$ . The black circles show the thermal wave decay described in (1).

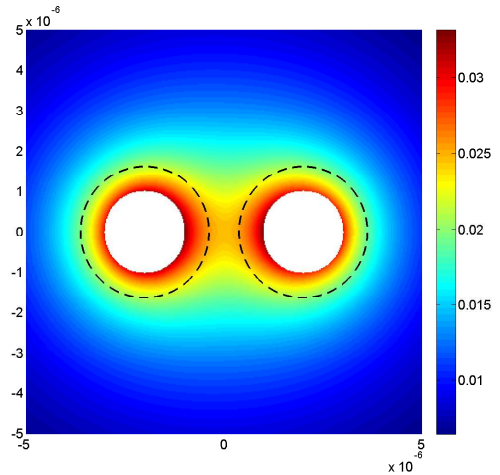


**Figure 6.** The thermal field of two particles,  $a = 1 \cdot 10^{-6}m$ ,  $b = 1 \cdot 10^{-6}m$  and  $d = 6a$ . The black circles show the thermal wave decay described in (1).

general angle of incidence in order to quantify these effects. This will provide a method for more accurately describing acoustic propagation in more higher concentration colloids than is given by current theories.

## 7. Acknowledgement

We are grateful to the UK Engineering and Physical Sciences Research Council (EPSRC) and Procter and Gamble for funding for this work through a CASE studentship for TAH.



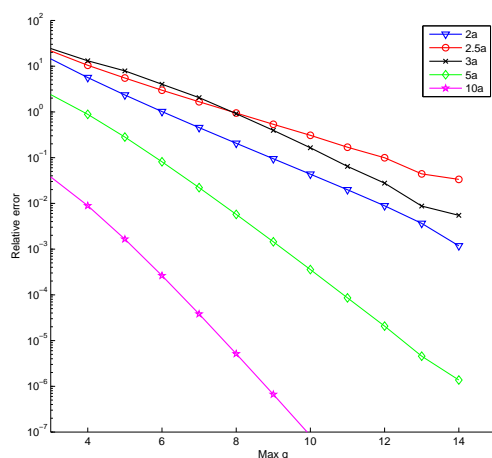


**Figure 7.** The error of  $A_{20}$  as a function for different distanced between the particles.

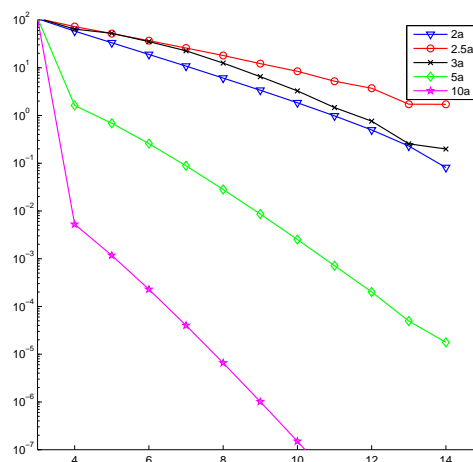


**Figure 8.** The error of  $A_{22}$  as a function for different distanced between the particles.

## References

- [1] Lord Rayleigh 1897 On the incidence of aerial and electric waves upon small obstacles in the form of ellipsoids or elliptic cylinders and on the passage of electric waves through a circular aperture in a conducting screen *Phil. Mag.* XLIV **266** 28-52
- [2] Epstein P S and Carhart R R 1953 The absorption of sound in suspensions and emulsions I. water fog in air *J. Acoust. Soc. Am.* **25** 553-65
- [3] Allegra J R and Hawley S A 1972 Attenuation of sound in suspensions and emulsions: theory and experiments *J. Acoust. Soc. Am.* **51** 1545-64
- [4] Lloyd P and Berry M V 1967 Wave propagation through an assembly of spheres 4. relations between different multiple scattering theories *Proc. Phys. Soc.* **91** 678-688
- [5] Gaunaud G C, Huang H and Strifors H C 1995 Acoustic scattering by a pair of spheres *J. Acoust. Soc. Am.* **98** 495-507
- [6] Harlen O G, Holmes M J, Povey M J W, Qiu Y and Sleeman B D 2001 A low frequency potential scattering description of acoustic propagation in dispersions *SIAM J. Appl. Math.* **61** 1906-1931
- [7] Harlen O G, Holmes M J, Povey M J W and Sleeman B D 2003 Acoustic propagation in dispersions and the geometric theory of diffraction *SIAM J. Appl. Math.* **63** 834-849
- [8] Harlen O G, Holmes M J, Pinfield V J, Povey M J W and Sleeman B D 2010 A perturbation solution for long wavelength thermoacoustic propagation in dispersions *J. Comput. Appl. Math.* **234** 1996-2002
- [9] Pinfield V J and Povey M J W 1997 Thermal scattering must be accounted for in the determination of adiabatic compressibility *J. Phys. Chem. B* **101** 1110-1112
- [10] Pinfield V J 1996 *Studies of Creaming, Occulation and Crystallisation in Emulsions: Computer Modelling and Analysis of Ultrasound Propagation* (PhD thesis, Procter Department of Food Science, University of Leeds)
- [11] Hemar Y, Herrmann N, Lemarchal P, Hocquart R and Lequeux F 1997 Effective medium model for ultrasonic attenuation due to the thermo-elastic effect in concentrated emulsions *J. Phys-Paris II*, **7** 637-647
- [12] Edmonds A 1957 *Angular Momentum in Quantum Mechanics* (Princeton U.P., London)
- [13] Kleinmann R E 1965 The Dirichlet problem for the Helmholtz equation *Arch. Ration. Mech. Anal.* **18** 205-229